Geology, Geophysics & Environment 2023, vol. 49 (1): 53–70

The fluid flow modeling procedure including a critically stressed fracture analysis of coalbed methane reservoir: a case study of Upper Silesian Coal Basin, Poland

Michał Kępiński[1], Paweł Ryder[2], Jacek Dudek[3], Daniel Podsobiński[4]

[1] *AGH University of Science and Technology, Faculty of Drilling, Oil and Gas, Krakow, Poland; PGNiG PKN Orlen, Exploration and Production Branch, Warsaw, Poland, e-mail: michal.kepinski@pgnig.pl (corresponding author), ORCID ID: 0000-0003-2309-4647*
[2] *PGNiG PKN Orlen, Exploration and Production Branch, Warsaw, Poland, e-mail: pawel.ryder@pgnig.pl*
[3] *PGNiG PKN Orlen, Exploration and Production Branch, Warsaw, Poland, e-mail: jacek.dudek@pgnig.pl*
[4] *AGH University of Science and Technology, Faculty of Drilling, Oil and Gas, Krakow, Poland; PGNiG PKN Orlen, Exploration and Production Branch, Warsaw, Poland, e-mail: daniel.podsobinski@pgnig.pl*

Received: 5 August 2022; accepted: 21 February 2023; first published online: 14 March 2023

Abstract: The geomechanical modeling turned out to be an essential component of the hydrocarbon exploration assisting reduction of risk of drilling issues and optimization of hydraulic fracturing treatment. This study provides a workflow of critically stressed fracture (CSF) analysis dedicated for coal layers. The main focus of the paper is applying the 1D mechanical models and following modelling of hydraulic fracturing treatment to describe the fracture behavior under the impact of the stresses at the wellbore scale. Another objective of presented study is demonstration of benefits of 1D and 3D CSF analysis to understand fracture contribution to gained volume of hydrocarbon after fracturing of coal seam. Interpretation of fracture orientation and their behavior is vital to effective development of coal bed methane (CBM) resources as the CSF can be responsible for considerable part of CBM production. Natural fractures and faults contribute to fluid flow through rock. It is often noted that natural fractures may not be critically stressed at ambient stress state. However, during stimulation the optimally oriented natural fracture sets have an inclination to become critically stressed. Hence, understanding of the recent stress state and fracture orientations is significant for well planning and fracturing design. The outcome of this study are comprehensive 1D mechanical Earth models (MEMs) for analyzed wells and explanation of behavior of identified CSF under variable stress state as well as understanding of the connectivity of natural fractures within zone subjected to fracturing treatment.

Keywords: coal bed methane, critically stressed fractures, fractures, fracturing treatment, Upper Silesian Coal Basin

INTRODUCTION

Geomechanical modeling (Fig. 1) has become a fundamental element of the hydrocarbon exploration process supporting the reduction of risk associated with instability and the designing of hydraulic fracturing treatment. An understanding of the mechanical properties of the reservoir is crucial for the optimal development of the oil/gas field. The grasp of these issues is particularly important in the case of complex static and dynamic models. The application of geomechanics provides insight into the relationship between natural fractures and stresses within a reservoir, which in turn has a direct correlation with the question of its productivity.

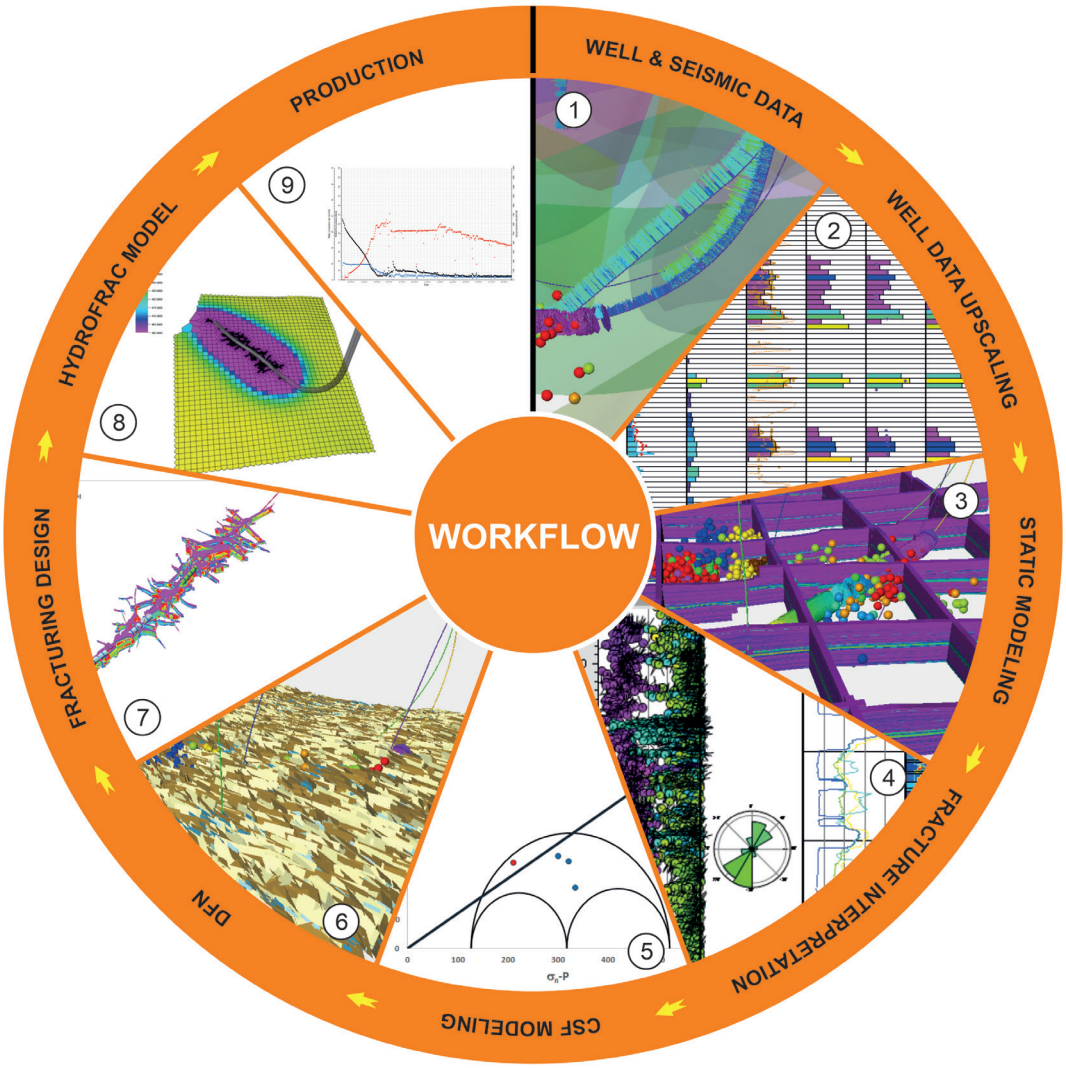

Fig. 1. *Applied workflow for the modeling procedure*

The objective of the following study was to test the potential of coal bed methane (CBM) in the Upper Silesian Coal Basin (USCB; Fig. 2). The main objective of the present study is to understand the fracture contribution during reservoir simulation for gas flow on example of this particular case. This approach is especially important in the case of CBM reservoirs, where permeability is mainly associated with a presence of natural fractures, which play a greater role in gas flow than the coal matrix itself (Dawson et al. 2011, Chatterjee & Paul 2012). Natural fractures and faults contribute to fluid flow through rock. Displacement on a fault or fracture surface is a mechanism that can prevent processes such as chemical or mechanical sealing and consequently can preserve permeability. Fluid flow in a fractured reservoir corresponds to the CSFs and faults. Therefore, to determine the stress state under which structures such as faults and fractures may be reactivated, it is necessary to identify the population of potentially permeable fractures (Barton et al. 1995). It has frequently been observed that natural fractures may not be critically stressed at the initial stress state. However, during stimulation the optimally oriented natural fracture sets have a tendency to turn into critically stressed sets (Zoback 2007). Therefore, knowledge of the recent stress state and fracture orientations is a substantial input for well trajectory planning and fracturing design.

The paper is organized so that the use of CSF in the context of CBM becomes clear to the reader with an emphasis on practical application in the realities of petroleum. The publication has the following structure: after the introduction, the authors discussed the methodology used and the built models. The basics of fracture analysis, as well as the concept of the CBM and the geological settings of the area of interest. Next, the results are discussed with particular emphasis on the production forecast. The area under study is located in the USCB with an area of 7,500 km², including 5,500 km² within Poland (Fig. 2). The basin was formed at the final stages of the evolution of the Moravo-Silesian Palaeozoic Basin and was developed in the Moravian-Silesian foreland of the Variscan orogene and became a part of its outer zones (Słoczyński & Drozd 2018). The USCB is characterized by a complicated geological setting due to its geological evolution containing two orogenic events – the Variscan and the Alpine (Zdanowski & Żakowa 1995).

The main target of CBM appraisal in the USCB is coal seam 510. This is due to the continuity of its occurrence and significant thickness. Seam 510 within the area of investigation (AOI) lies at a depth of approx. 1,600 m in the northern part to 700 m in the south-eastern direction in the vicinity of the Jawiszowice Fault, with dip angles ranging from 5 to 20°. The interpretation of 3D seismic shows that the structural strikes of the layers are approximated to the NW-SE and NE-SW directions. Within the AOI, seam 510 was drilled in 10 wells. The average seam thickness is 5.36 m and ranges from 3.7 to 7.1 m. It reaches the greatest thickness in the eastern part of the area, which is documented by the M-4 well. Kotas et al. (1990) estimated CBM resources in the USCB at 365 billion m³.

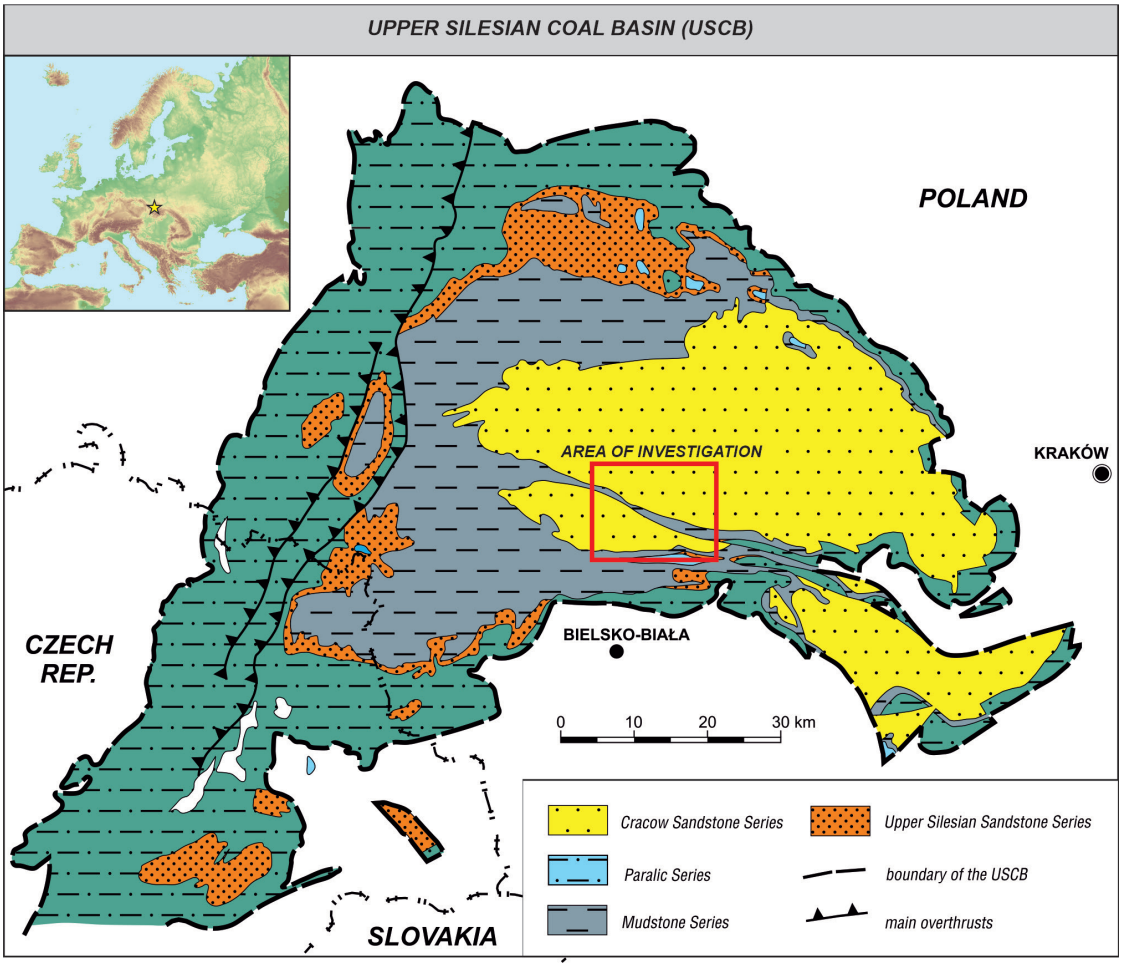

Fig. 2. *Geological map of the USCB showing the area of investigation (AOI) (after Jureczka et al. 2019)*

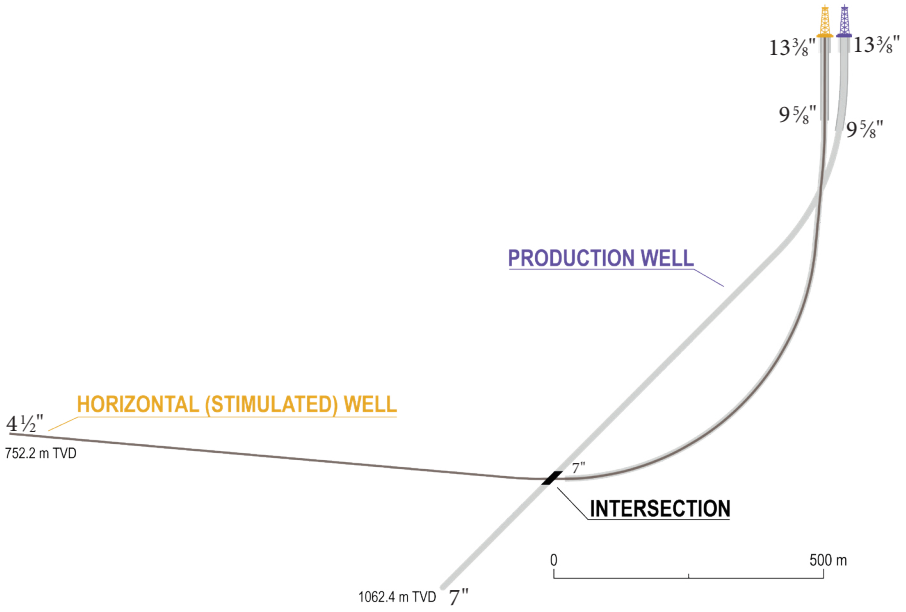

Fig. 3. *Heel intersection system of G-3K and G-4H wells*

Recent works conducted by PGNiG (ORLEN Group) in the region have been focused on CBM projects which are strongly dependent on extensive geomechanical studies. Such an approach is dictated by drilling methods which rely on the construction of well doublets in the "heel intersection system" (Fig. 3).

The reason for drilling wells in the configuration presented was to perform stimulation treatments in a horizontal well (multi-stage plug-and-perforate hydraulic fracturing) in order to enhance well drainage and improve the natural fracture network, whereas the intersecting deviated well was used for production purposes. An electrical submersible pump (ESP) was used for artificial lift performance which would have been impossible to implement in a horizontal well because of the large deviation angle.

One of the most common phenomena in a CBM reservoir is the variable coal permeability due to combined stress and matrix shrinkage. These two effects compete with one another, and the dominance of either effect depends on the coal properties and reservoir change. Palmer & Mansoori (1998) described the ratio of porosity at a given pressure to initial porosity using the described reservoir compressibility in the dynamic model. All of these factors have a significant impact on well productivity and estimated ultimate recovery (EUR).

METHODS AND MODELS

Static model

The first step of analytical works was focused on structural grid construction. The structural framework (Fig. 4) was built using 3D seismic horizons, fault interpretation and well stratigraphy. The great advantage of the modeled area is a relatively good imaging of the tectonic features as faults were recognized on seismic, microresistivity image logs and microseismic data. The modeled volume covered an approx. 95 m thick Upper Silesian Sandstone Series (USSS) and upper part (50 m) of the Paralic Series (PS). Applied lateral and vertical cell dimensions are 50 × 50 and 1 m respectively.

The facies model was generated using truncated Gaussian simulation (TGS) of three predominant rock types. TGS algorithm (Matheron et al. 1987) is intended for depositional models characterized by a constant and ordered succession of facies. The simulation truncates single Gaussian random field into domains, that are determined by expected rock patterns (Labourdette et al. 2008). The upscaled (Fig. 5) coal fraction (7.49%) in the model is coherent with the average percentage of coals with a thickness exceeding 1 m (7.63%) in USCB.

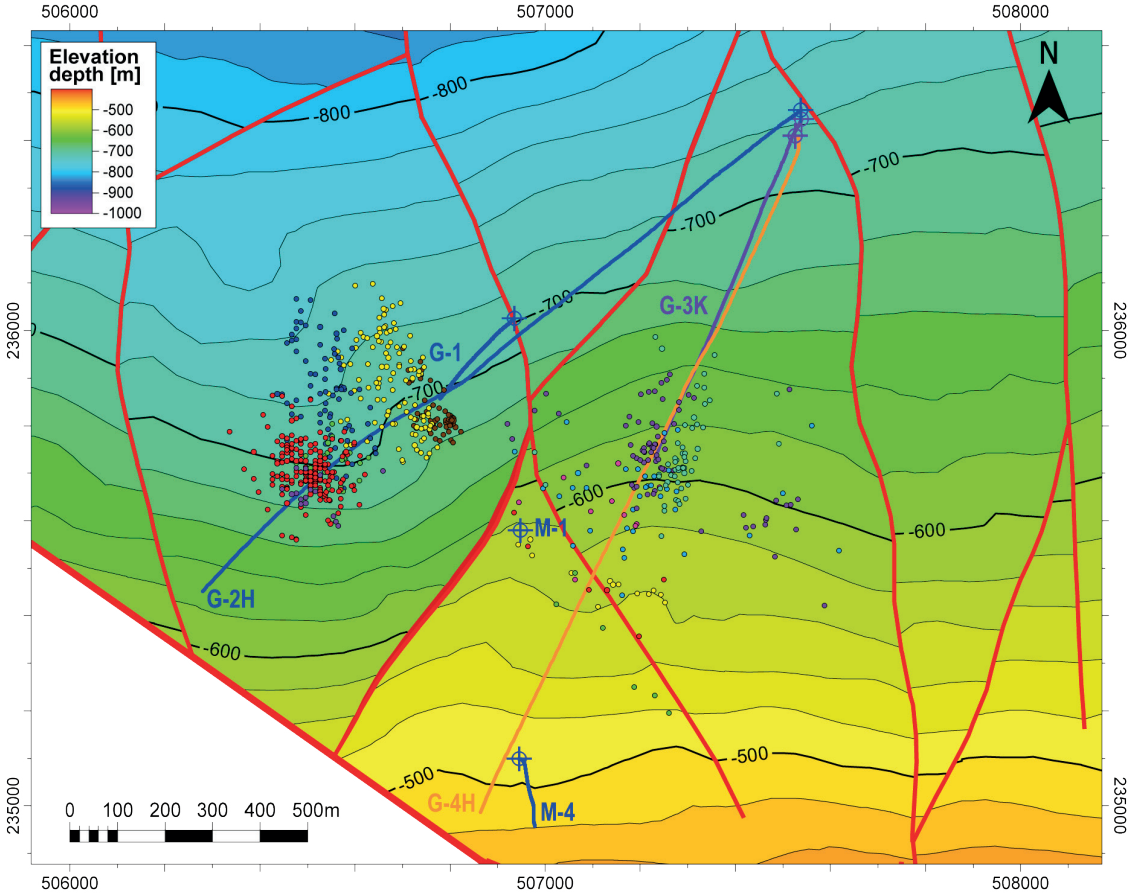

Fig. 4. *Structural map of the base of coal bed no. 510; microseismic event colors refer to different stages*

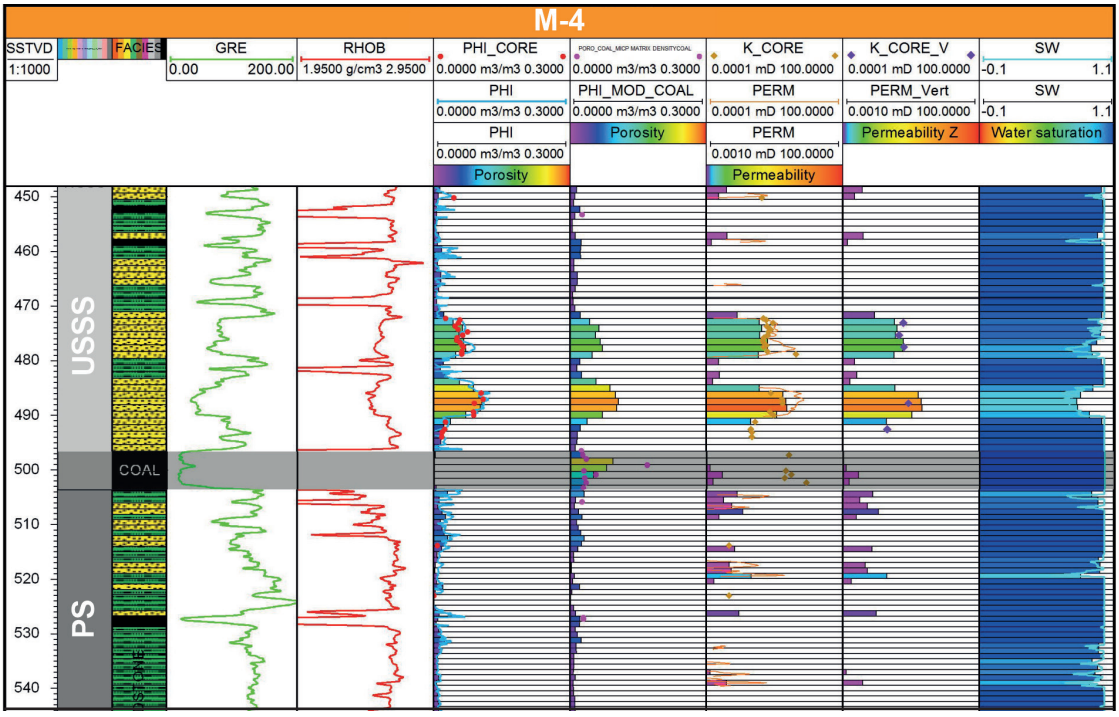

Fig. 5. *Upscaling results showing the petrophysical properties of the interpreted rock types from M-4 well*

Property models (Figs. 6, 7) were created using Gaussian random function simulation based on data comprising core calibrated well log interpretation. The well log interpretation was calibrated to the mercury injection capillary pressure (MICP) data to reflect most accurately the properties of the coal and surrounding rock types. The petrophysical properties were simulated using facies-specific distribution including the following:

– effective porosity,
– horizontal and vertical permeability,
– water saturation.

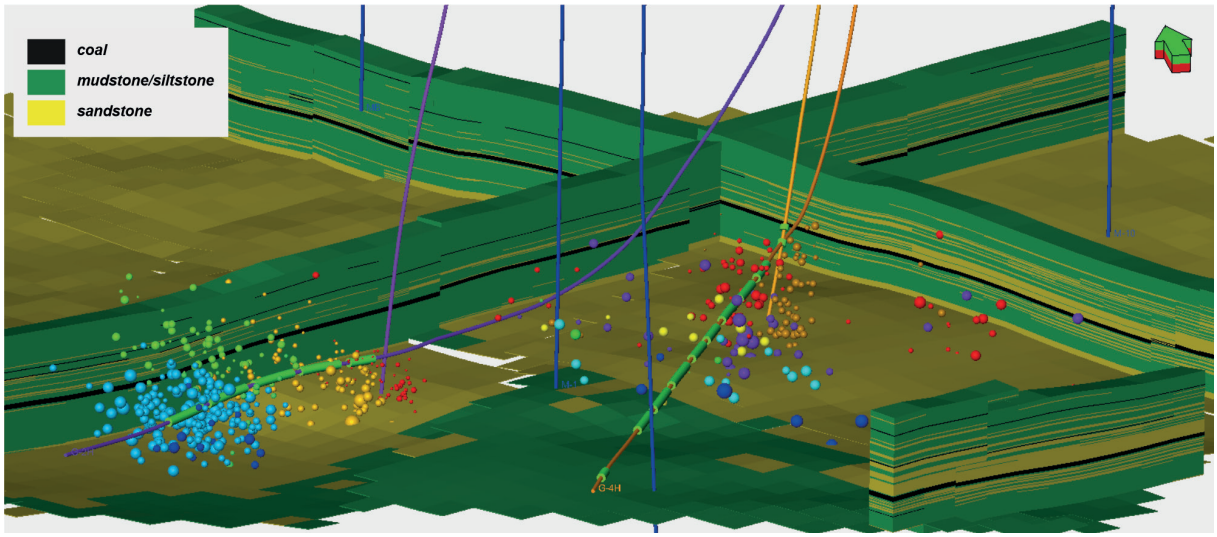

Fig. 6. *3D view of the well trajectories, the microseismic events and facies model for coal bed no. 510 and surroundings; microseismic event colors refer to different stages*

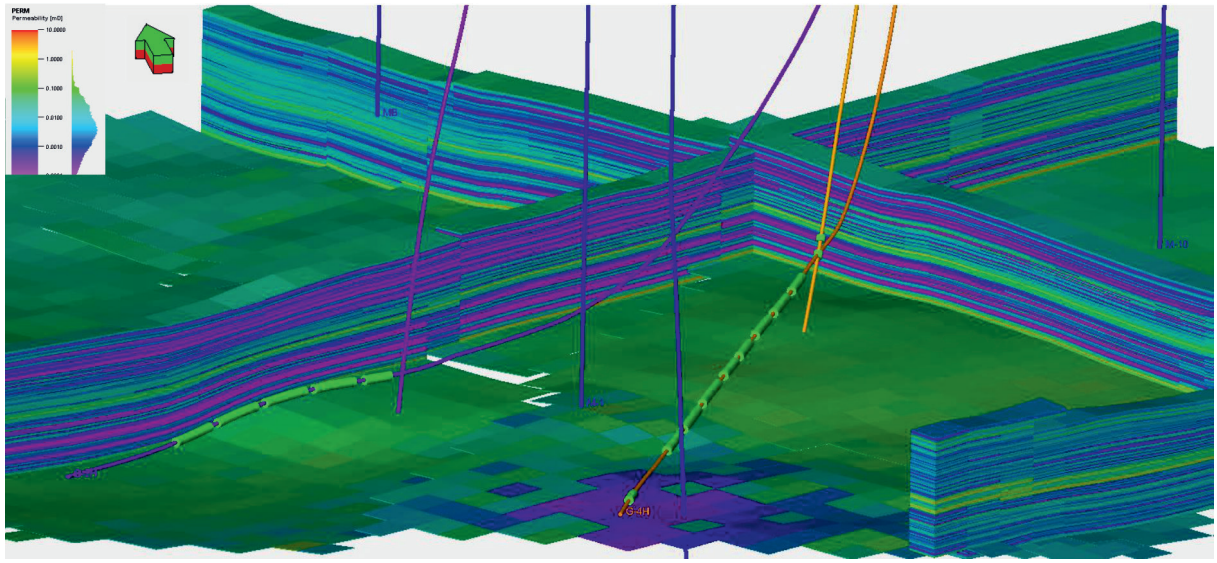

Fig. 7. *3D view of the permeability model for coal bed no. 510 and surroundings*

The properties of the key coal bed no. 510 (Fig. 8) core sample from M-4 well are listed below (core analysis commissioned by PGNiG and provided by Oil and Gas Institute – National Research Institute):

- MICP permeability matrix mean: 0.3 mD,
- MICP fracture permeability: 2–3 mD,
- porosity (avg.): 3.9%,
- coal thickness: 4.9–7.0 m,
- CH_4 content: 9–14 m^3/t,
- world classification (ASTM D388-18): most are hvAb (high-volatile A bituminous),
- Polish classification: bituminous coal C,
- ash content: 1.55–4.85% (very low),
- vitrinite content (avg.): 27–97% (64%).

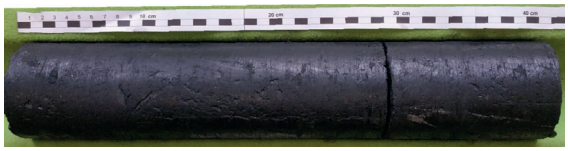

Fig. 8. *Coal no. 510 core sample from M-4 well*

Fracture analysis

An understanding of the factors that govern the characteristics of fracture patterns, such as orientation distribution, density, spatial variation and chronology is fundamental to improving the methods used to characterize fractured reservoirs (Ahmadhadi et al. 2008). The discrete fracture network (DFN) workflow (Schlumberger 2008) is used to realistically model the dynamic behavior of the fractures that give rise to reservoir-scale and well-scale non-continuous flow behavior. A DFN model typically combines deterministic and stochastic discrete fracture data (Dershowitz et al. 1998).

Natural fractures and faults contribute to fluid flow through rock. Displacement on a fault or fracture surface is a mechanism that can hinder such processes as chemical or mechanical sealing and consequently can preserve permeability. Fluid flow in fractured reservoirs corresponds to CSFs and faults and is oriented approximately 30° to the $S_{H\max}$ direction (Rogers 2003). Hence, the determination of the stress state under which such structures as faults and fractures could be reactivated is of non-negligible value in the identification of the population of potentially permeable fractures (Zoback 2007). It has been frequently observed that natural fractures may not be critically stressed at the initial stress state. However, during stimulation the optimally oriented natural fracture sets have a tendency to turn into critically stressed sets. Therefore, the understanding of the recent stress state and fracture orientations is a substantial input for well trajectory planning and fracturing design.

To apply the concept of critical stress to fracture flow, the *in situ* stress field acting along all faults and fractures in a given rock volume can be decomposed into shear and normal stress components (Sathar et al. 2012). As soon as the magnitude and direction of the stress field has been constrained, the shear stress (τ) and normal stress (σ_n) acting on a fracture surface can be stated by following equation (Jaeger et al. 2007):

$$\tau = \beta_{11}\beta_{21}\sigma_1 + \beta_{12}\beta_{22}\sigma_2 + \beta_{13}\beta_{23}\sigma_3,$$

$$\sigma = \beta_{11}^2\sigma_1 + \beta_{12}^2\sigma_2 + \beta_{13}^2\sigma_3,$$

where β_{ij} are the direction cosines between the fracture surface and the stress tensor and σ_1, σ_2, and σ_3 is the magnitude of the maximum, intermediate, and minimum principal stresses, respectively. Faults and fractures are in a critically stressed state and therefore likely to be conductive when scatter above the Mohr–Coulomb failure envelope and when the shear stress and normal stress on their surfaces are plotted with respect to the *in situ* stress field in a Mohr space (Fig. 9) (Sathar et al. 2012). The source of uncertainty is the fact that faults and fractures perturb the stress field so that the far-field stress is not necessarily representative in an intensely fractured rock volume.

The evaluation of fracture stability was performed using a Fracture Stability plug-in for Techlog based on an analytical approach implementing the Mohr–Coulomb shear failure criterion. Earlier prepared mechanical Earth models (MEMs) were used as input for fracture stability analysis. The MEMs for the wells under study were built in six steps using log measurements and well testing data (Kępiński 2020). MEMs were computed in Techlog 2019.1. Several findings obtained from the drilling reports provide constraints for the MEMs.

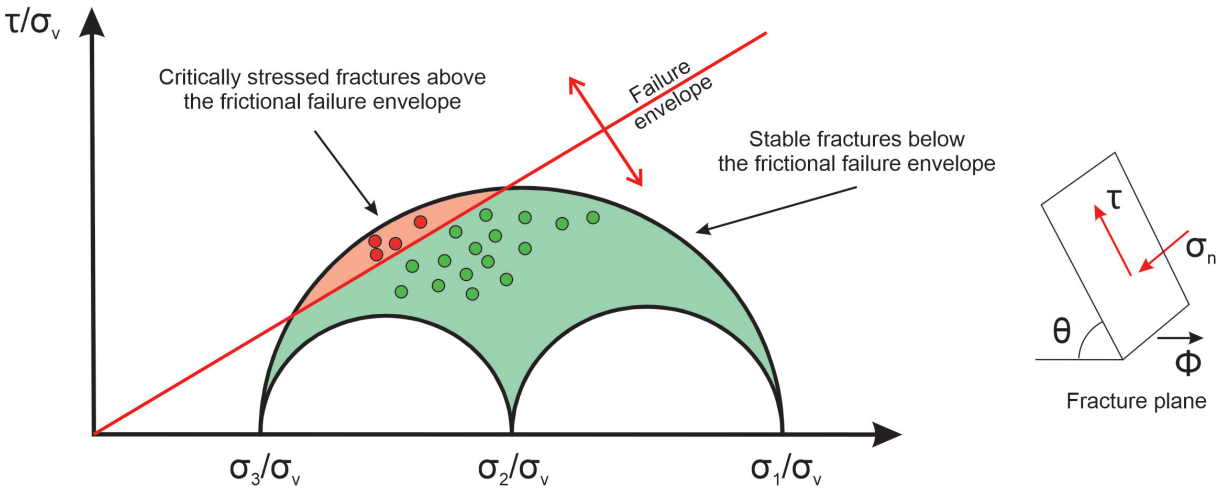

Fig. 9. *Theory of critically stressed fractures (adapted from Barton et al. 1995, Rogers 2003, Jaeger et al. 2007, Sathar et al. 2012). Mohr's circle for a spatial stress state represents the shear stress and the normal stress acting on the fracture plane in response to the actual stress field. Dots represent exemplary fracture orientations.* σ_n *– effective normal stress,* Φ *– azimuth with respect to stress field,* θ *– dip,* τ *– shear stress*

The horizontal stress profiles of the wells analyzed were determined using the presented workflow; their outputs were checked against the interpreted compressive and tensile wellbore failures. The stress boundaries model, poro-elastic horizontal strain model and effective stress ratio approach, coupled with an analysis of wellbore failure (Zoback et al. 2003, Zoback 2007), were used to derive continuous stress profiles. Using this approach, the stress measurements carried out using different methods could be compared, providing a reliable assessment of the stress state, which is an essential element for planning future projects in the region.

Dips and azimuths of the fracture dataset comprise features identified through the interpretation of CMI (The Weatherford Compact™ microimager) images. A classification of fractures was performed on the basis of their various instrument responses (darker or lighter than the background formation or matrix) (Milad et al. 2018). Also, the fractures/faults were determined as terminated and truncated features (incomplete sine waves of bedding and fractures) to support the fracture timing and geometry interpretation, as well as the sediment body analysis.

A tectonic stress direction analysis was performed in a vertical section of a near offset well (G-1), where the effect of borehole inclination is small and can be neglected. In this well, the induced fractures were observed and used as a maximum *in situ* stress indicator. The $S_{H\max}$ direction, as the induced fractures indicate, is NW-SE. The main direction of the fully sinusoid fractures picked on the G-4H well is aligned with the maximum *in situ* stress direction.

In the G-4H well, induced fractures and the tensile region were identified as the possible *in situ* tectonic stress direction indicators. However, their direction cannot be used as *in situ* stress direction indicators due to their deviation from the vertical. Under such circumstances, the relation describing the location of breakouts and drilling induced tensile fractures becomes non-linear and sensitive to the relative magnitudes of the principal stresses.

Using the current data set, and keeping the above-mentioned uncertainties in mind, a critically stressed fracture analysis was performed mainly for two cases, i.e., for ambient conditions and for conditions modified by stimulations. It has been consistently observed that natural fractures may not be critically stressed at ambient conditions. However, once stimulated, the optimally oriented natural fractures tend to become critically stressed, and hence conductive. At approx. 11 MPa, injection fractures become critically stressed (150° of $S_{H\max}$ direction were used) (Fig. 10).

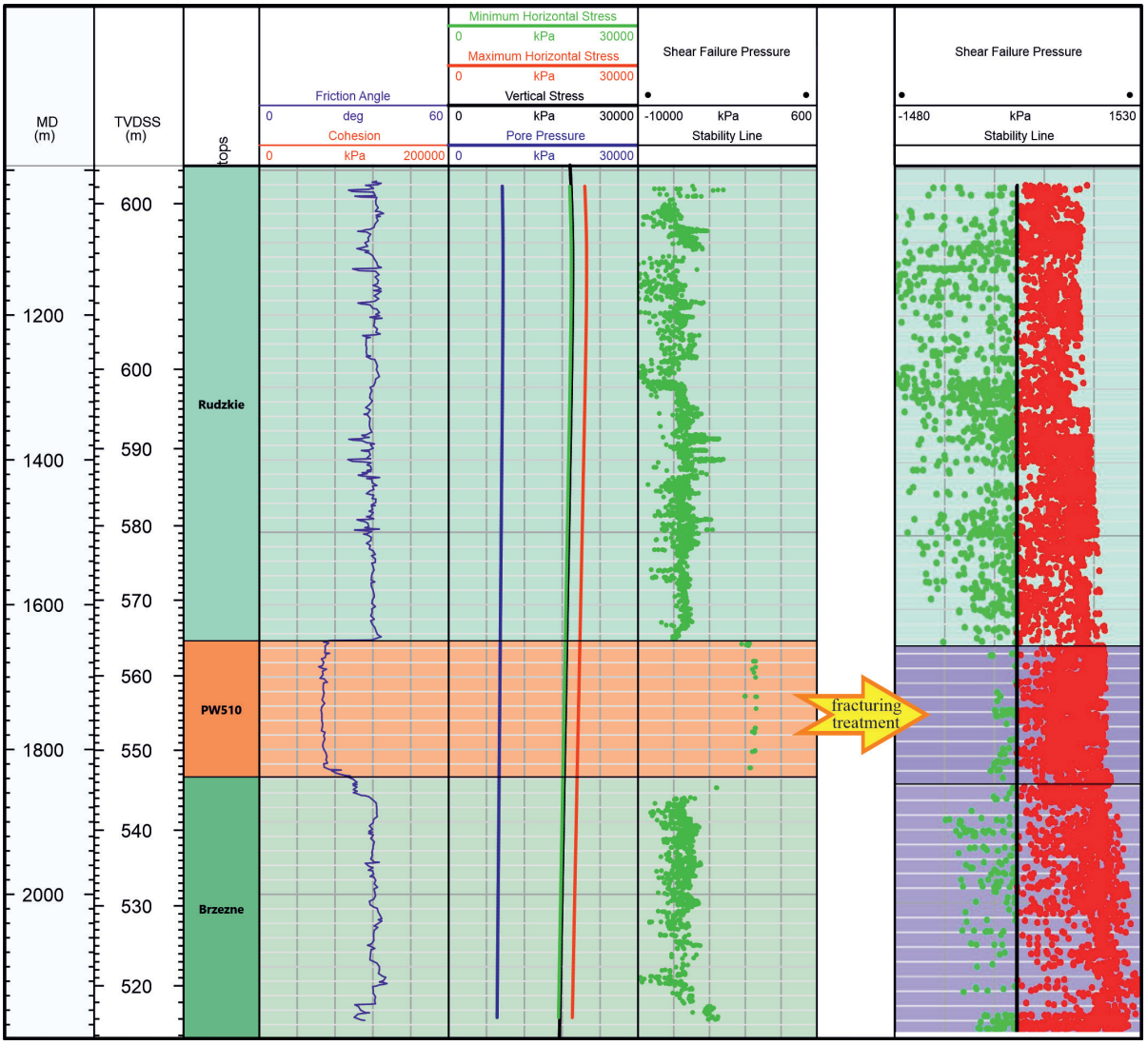

Fig. 10. *At ambient conditions no fractures seem to be critically stressed. Fractures become critically stressed after fracturing treatment. On the third track, the failure values are displayed for each of the fractures analyzed (green – not critically stressed, red – critically stressed (the baseline represents the failure line)*

When production starts the stress perturbation caused by the fracture treatment gradually decreases following pressure drop.

Based on the analysis of the current data set (Fig. 11), the natural fractures with a tendency to be critically stressed are the NW-SE and NE-SW striking fractures (Fig. 12). A fracture modelling job was carried out using Petrel software and image logs data in order to obtain new information about the fracture system in this field.

The discrete fracture network (DFN) workflow was used to realistically model the dynamic behavior of the fractures that gave rise to reservoir-scale and well-scale non-continuous flow behavior. Resistive fractures were filtered out. The remaining conductive fractures were divided into four sets, including cleats within coal seams. Fracture orientations from the wells correspond with the neighboring coal mine observations. On the basis of the loaded fracture interpretation, the fracture intensity logs P32 (area of fractures / volume of rock mass) [L-1] for each set were established, scaled up to the static model grid resolution using the neighbor cell method and simulated by petrophysical modeling (Gaussian random function simulation) into the previously built 3D geological framework model (Ahmed Elfeel & Geiger 2012).

An additional deterministic frac set was generated from fault interpretation and the fracture set associated with its fault zones.

In the course of upscaling the fracture properties for dual porosity simulation, the knowledge of fracture apertures and permeability was applied. Fracture permeability was calculated using cubic law on the basis of exponential distribution of apertures (mean: 0.00002 m, min. 0, max. 0.001) in Petrel 2019.1. This is an application of Darcy's law of flow through the fractures and assumes flat and smooth fracture plane (Schlumberger 2021).

For well-populated cells, the permeability tensor was computed using the Oda algorithm (Snow 1969, Oda 1985). Due to the fact that modeled permeability distributions have to match the effective permeability from production data, this attribute was iteratively adjusted. The DFN model (Fig. 13) created was incorporated into the process of hydraulic design and its further optimization.

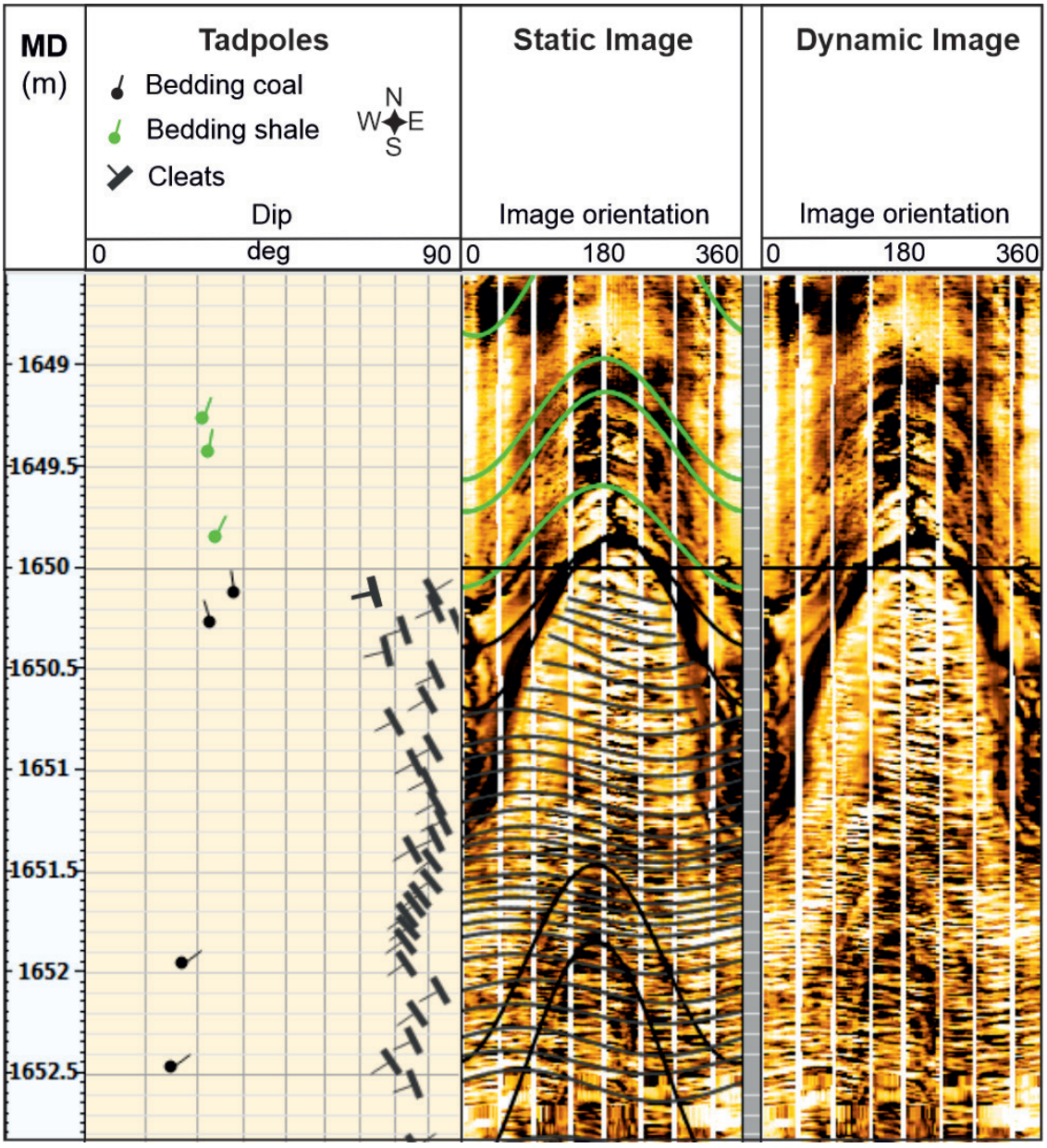

Fig. 11. *Fracture interpretation on image log from G-4H well (sample interval)*

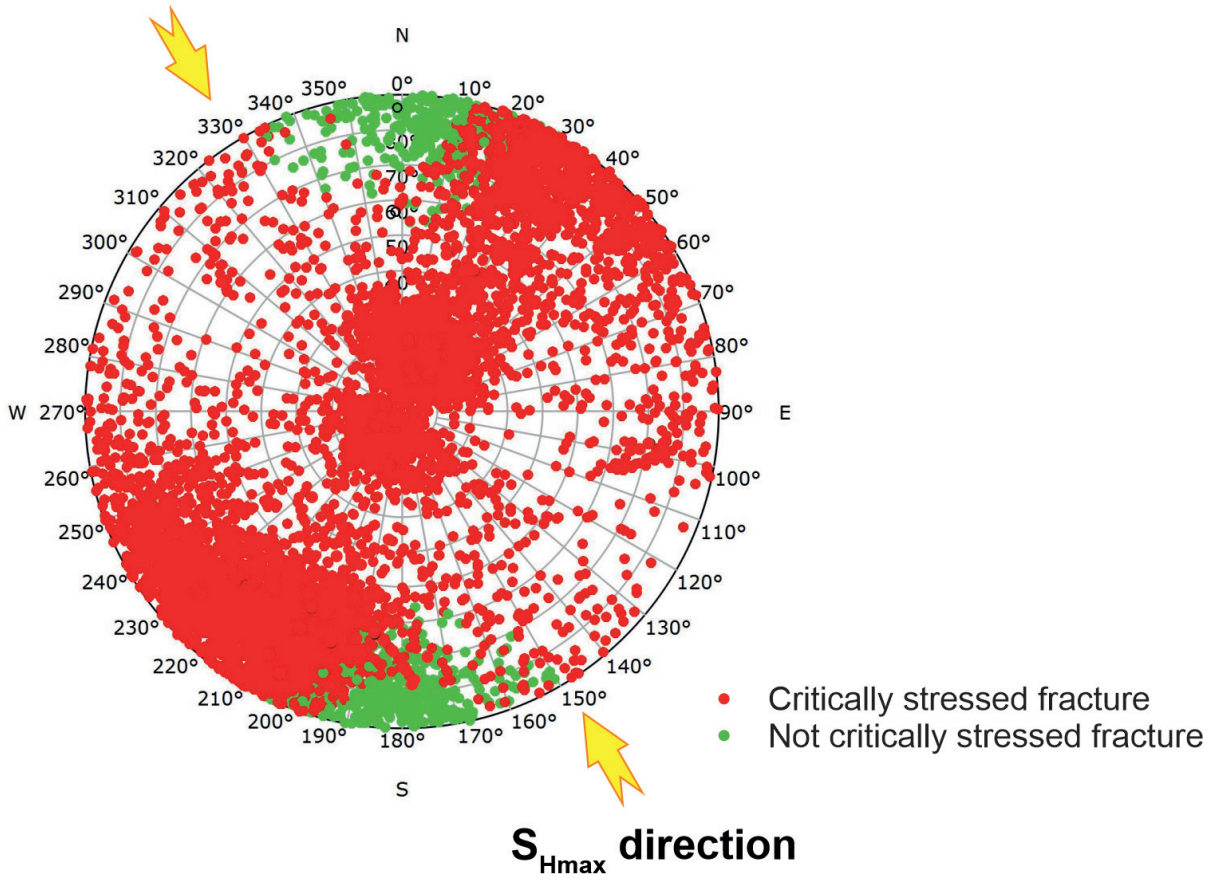

Fig. 12. *The stereonet plot with fracture orientations (pole to plane) – stress state after fracture stimulation*

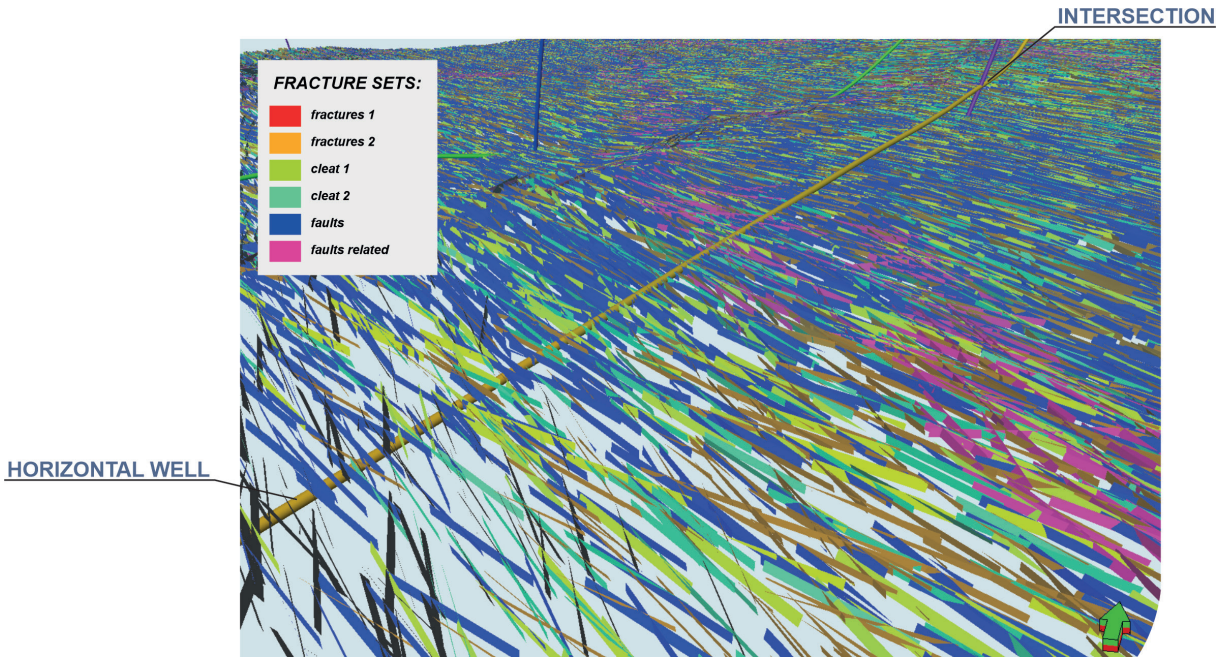

Fig. 13. *A section of the model showing the discrete fracture network generated using deterministic approach. Fracture sets 1 and 2 are not frequent compering to cleats*

Microseismic

Microseismic monitoring (Fig. 14) allowed for the observation of two major fracture trends: the primary azimuth: ~150° associated with the S_{Hmax} direction, and the secondary azimuth: ~130° most likely related to natural fractures or fault reactivation – which complies with the interpreted cleat and fracture sets from the microimager. There is some uncertainty connected with lack of microseismic events towards Variscan, SSW-NNE trending faults. This situation may be explained by existence of potential barriers characterized by limited fracture conductivity.

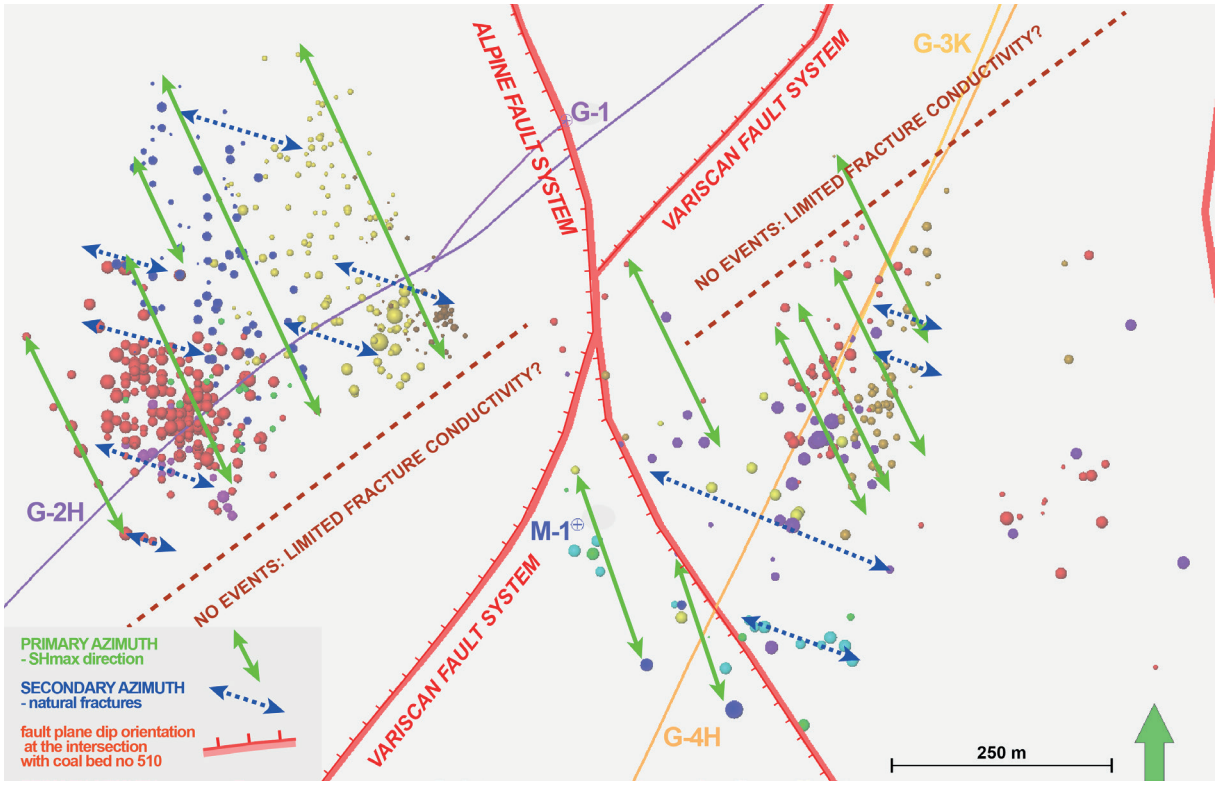

Fig. 14. *Interpretation of microseismic events*

Dynamic model

The coal deposits are an unconventional type of reservoir in which coal is at the same time the source and reservoir rock for methane. This formation is characterized by a dual porosity system where the majority of the gas is stored by adsorption phenomena in an almost impermeable microporous matrix. On the other hand, there is a natural fracture network which stores relatively low volume of methane and is primarily occupied by water (Stopa & Mikołajczak 2018).

Gas production from CBM formation is divided into three main flow mechanisms: gas desorption from the matrix, gas diffusion from the microporous coal matrix to the fracture system and the flow through the fracture network to the wellbore. The main gas flow mechanism in coal formation is the Langmuir adsorption model – basic input to the CBM reservoir model. A typical sorption isotherm shows initial reservoir gas content vs pressure, critical desorption pressure and abandonment conditions. Gas will not flow until reservoir pressure is lower than critical pressure. For Polish CBM study purposes, comprehensive lab tests commissioned to Geokrak on the rock samples were performed (Wronka & Basta 2019), finally allowing for an estimation of the Langmuir isotherm (Fig. 15) with its further implementation into the dynamic reservoir model.

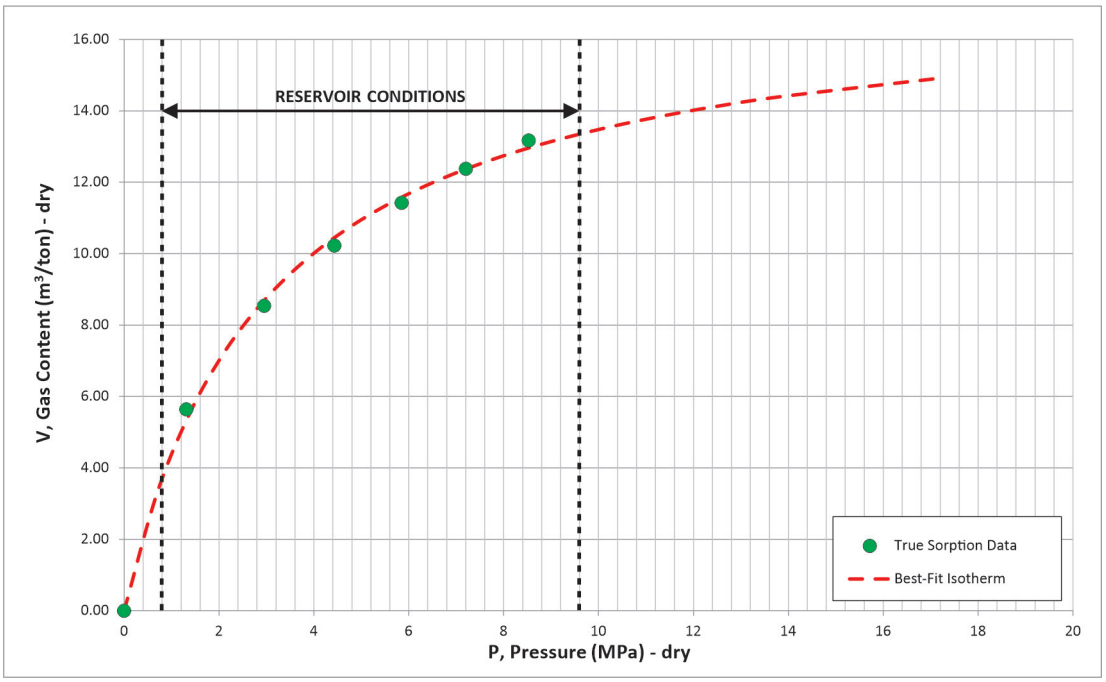

Fig. 15. *Langmuir model applied into the dynamic reservoir model (sorption data commissioned by PGNiG for samples from M-4 well acquired by Geokrak laboratory)*

These specific production phenomena provide the reason for the significant difference between the production strategy of CBM reservoirs and conventional ones. The first stage of production is the dewatering of the formation. Before the gas in a CBM reservoir flows through the media, it has to overcome the threshold pressure, which is defined as the minimum pressure needed to initiate the displacement of a wetting phase by a non-wetting phase from a porous medium 100% saturated with the wetting phase (Zheng & Xue 2011). Unfortunately, because of poor reservoir quality and insufficient micropore connections, the simple vertical or even horizontal wells cannot produce gas with commercial rates. Therefore, the crucial part of the development process is to maximize the inflow to the well from the reservoir. One of the most popular production intensification methods is hydraulic fracturing. However, due to CBM reservoir specificity, it differs significantly from conventional treatment. In order to minimize failure, special care must be taken during the stimulation design process which involves using the most advanced geomechanical analyses (Reynolds & Shaw 2005, Xuanhe et al. 2019). Therefore, for this study purposes the hydraulic fracturing treatment design and optimization process was conducted in the most advanced commercial hydraulic fracturing simulator – Kinetix (Schlumberger 2022). This tool, being a plugin to the Schlumberger Petrel Platform integrates geological, petrophysical, completion engineering, reservoir engineering, and geomechanical data in a repeatable workflow that ensures data integrity and high decision quality.

Integration all of the above models into a single study allowed Authors to simulate the full scale stimulation treatment that have been conducted in CBM reservoir preserving all of its assumptions as plug and perf technology, hydraulic fluid and proppant type & volumes, number of stages etc. As a result, it was possible to implement the effects of the treatment into the dynamic model as transmissibility multipliers (Fig. 16), which mimic the created fractures with their approximate shape, direction, size and proppant concentration (final conductivity). Moreover, basing on well test data the authors assumed the fault zones to be impermeable, which has been confirmed by the analysis of microseismic events.

In order to enhance dynamic simulation performance, the authors decided to introduce a simplified fracture model based on the local-grid-refinement (LGR) technique (Fig. 17). Based on the obtained fractures parameters they changed very detailed unshaped grid into equal grid-blocks with averaged transmissibility values.

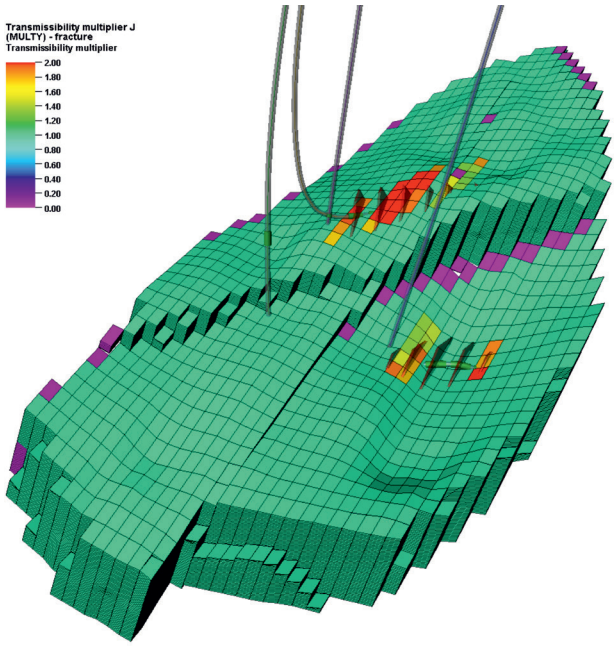

Fig. 16. *Fracture transmissibility multiplayer for coal bed no. 510 and surroundings – the averaged effect of hydraulic fracturing. Pink grid blocks – impermeable zones, green grid blocks – zones with very low reservoir permeability, red-yellow grid blocks – high-permeable zones after hydraulic fracturing treatment. Lateral and vertical cell dimensions are: 50 × 50 and 1 m respectively*

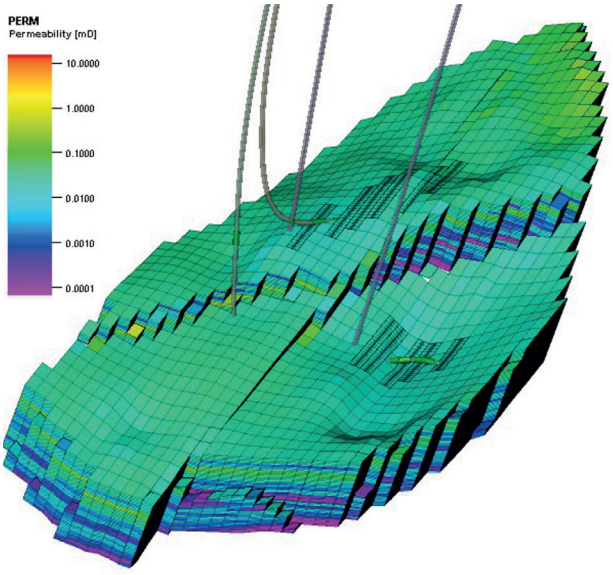

Fig. 17. *Matrix permeability with hydraulic fractures marked as LGR (local grid refinement) for coal bed no. 510 and surroundings. Lateral and vertical cell dimensions are: 50 × 50 and 1 m respectively*

Subsequently, utilizing the obtained results, the simplified fractures were deployed into the dynamic model (red boxes/plates) (Fig. 18) and dynamic CBM reservoir model was initialized.

Initially, water (blue) filled the entire volume of the formation and fractures except for the coal matrix with the absorbed methane (red). Because of pressure drop process (due to water production), the previously absorbed methane begins to desorb into the facture network, which is the main means of the transportation of gas. This process can be clearly seen as a reduction in water saturation (Fig. 19).

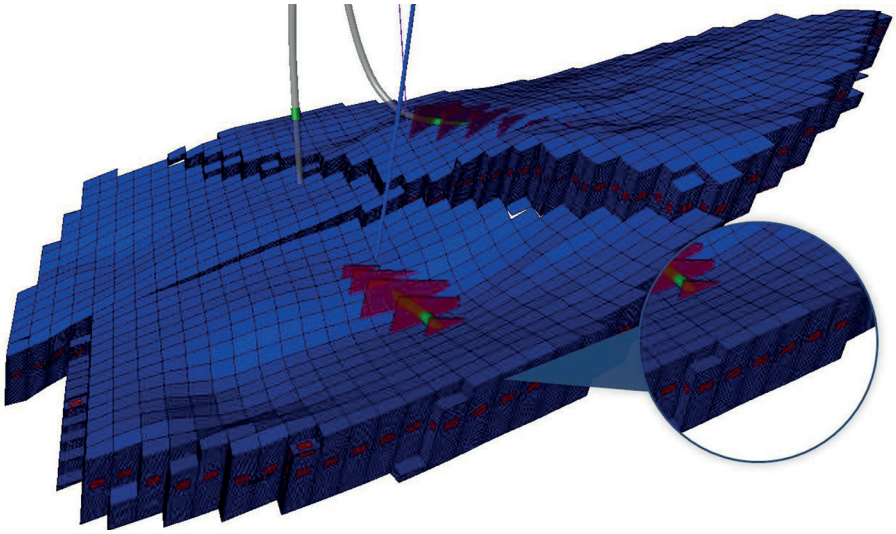

Fig. 18. *Water saturation at the start of simulation for coal bed no. 510 and surroundings. Blue color – grid blocks saturated with water, red plates – simplified hydraulic fractures, red cuboids – grid blocks matrix filled with absorbed methane. Lateral and vertical cell dimensions are: 50 × 50 and 1 m respectively*

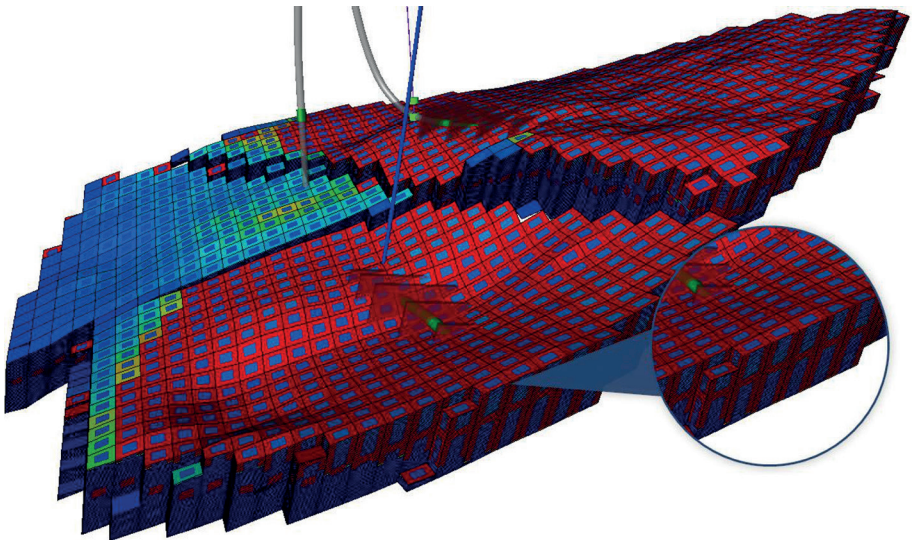

Fig. 19. *Water saturation at the end of simulation for coal bed no. 510 and surroundings. Blue color – desaturated matrix filled with water, red plates – simplified hydraulic fractures, red grid blocks – fractures filled with desorbed methane. Lateral and vertical cell dimensions are: 50 × 50 and 1 m respectively*

Production forecasts

As a first step of production forecasts preparation, the dynamic model was calibrated to the available historical data – the long-term production test. For the first production well, the testing period lasted more than two years and for the second – almost a year (2 production periods, 2 build-ups). Both wells were equipped with permanent downhole pressure gauges which substantially increased the quality and reliability of performed calibration process. To calibrate the model, an iterative process of fitting the parameters was performed. The main calibrating parameters were: the intensity, porosity and permeability of fractures, fault transmissibility, as well as hydraulic fracture conductivity. As can be observed in the figure below (Fig. 20), the authors of this paper obtained a fairly good history match of all the main parameters – the bottomhole pressure, gas production rate, water production rate, all of which were in an acceptable range.

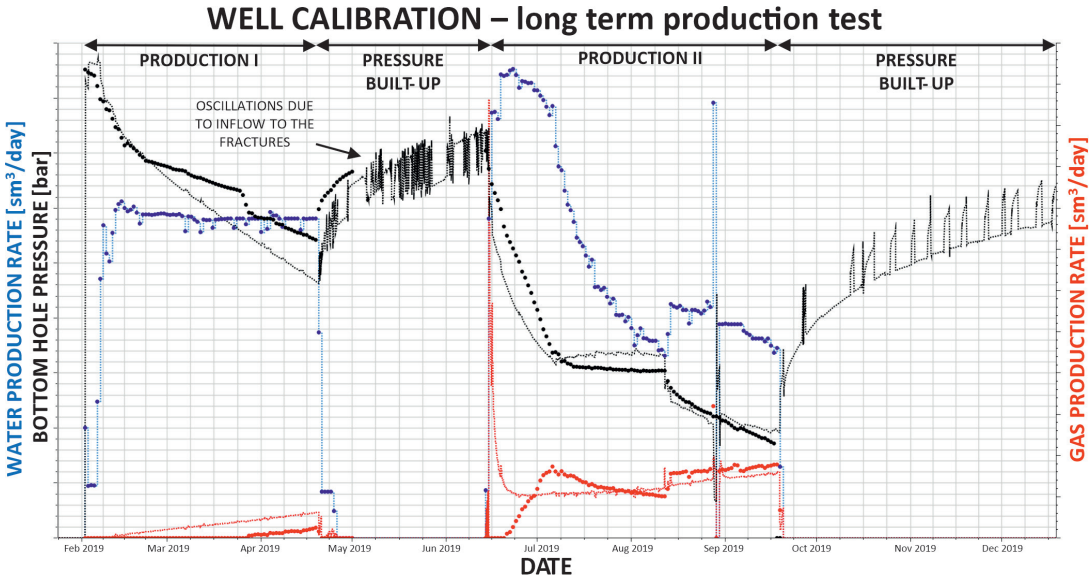

Fig. 20. Obtained history match – dots: measured data; curves: dark-colored – bottomhole pressure, blue – water, red – gas. Values on the axes was hidden due to confidentiality

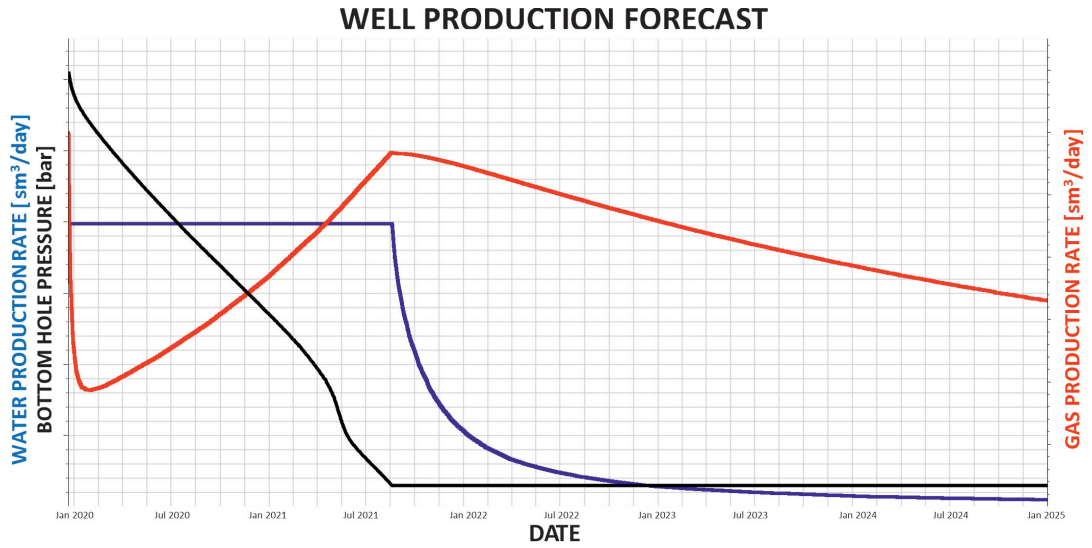

Fig. 21. Production forecast results for the second well – indicated by curves: dark-colored curve – bottomhole pressure, red – the gas rate, blue – the liquid flow-rate. Values on the axes was hidden due to confidentiality

All of the discrepancies between the simulated and historic data mainly came from the high level of complexity of the post-multi-fracturing model. For very heterogenic and low permeable CBM reservoirs it is almost impossible to ideally mimic fracture propagation and its final transmissibility being dependent on uneven proppant concentration, etc. In this case, authors used simple fracture models that brought local abrupt changes in reservoir parameters that led to big permeability/transmissibility contrasts. The impact of this phenomena can be seen during the build-in pressure periods, where its value oscillates in the course of pressure stabilization (last part of the dark curve).

The results presented on the graph (Fig. 21) accurately reflect the typical CBM production period. The first period is dewatering of the formation connected with a decrease in reservoir pressure and the start of desorption of gas from the matrix. Consecutively, gas flows through the fracture network to the wellbore until it reaches the peak of production and then decreases similarly as in a conventional reservoir.

SUMMARY AND CONCLUSIONS

Based on the analysis of the current data set, the fractures of the NW-SE and NE-SW strikes can be seen as the most optimal in the modelled stress field. The conclusion to be drawn from the interpretation of the image log is that the most frequently connected and conductive fracture set is the NW-SE strike. Thus, in this part of the USCB horizontal and inclined wells drilled to the NE-SW azimuth, a maximum number of optimally oriented natural fractures would tend to intersect, if only they occur and are effectively connected away from the wellbore. The breakouts, drilling-induced fractures and microseismic monitoring show consistent $S_{H\max}$ direction across all wells. There was no possibility to distinguish flowing from closed fractures due to lack spinner log or other.

A proper model of the fracture network and consequent fracturing treatment are crucial for obtaining accurate results of dynamic simulation.

The work of the authors of this paper was used as a basis for developing a dynamic model of the fractured CBM reservoir into which the results of the fracturing treatment were implemented. The results obtained (Fig. 21) properly mimic the behavior of real field data, thereby allowing for the generation of a reliable CBM production forecast. On the other hand, even with a most detailed history match, due to the number of assumptions made, as well as uneven fracture propagations and the lack of CBM reservoir analogs, the forecasts performed will be biased and will be tainted by a great level of uncertainty. The variables with the greatest uncertainty include the proppant concentration, fracture distribution, aperture, length, and final conductivity. The analysis proves that hydraulic fracturing treatment is necessary for natural fractures to become critically stressed and hence conductive. Without the stimulation treatment it is not possible to obtain gas desorption from the coal matrix and make flow possible.

The authors wish to thank PGNiG SA for its permission to publish this paper. Special thanks are dedicated to reviewers K. Czuryłowicz and S. Matthai for their constructive and helpful comments and corrections. We also thank A. Świerczewska for her significant contribution to improving the text of the article. The help of L. Berezowski in improving the English text is much appreciated.

REFERENCES

Ahmadhadi F., Daniel J.-M., Azzizadeh M. & Lacombe O., 2008. Evidence for pre-folding vein development in the Oligo-miocene Asmari Formation in the Central Zagros Fold Belt, Iran. *Tectonics*, 27, TC1016. https://doi.org/10.1029/2006TC001978.

Ahmed Elfeel M. & Geiger S., 2012. Static and dynamic assessment of DFN permeability upscaling. [in:] *SPE Europec/EAGE Annual Conference, June 4–7, 2012, Copenhagen, Denmark*, SPE-154369-MS. https://doi.org/10.2118/154369-MS.

Barton C.A., Zoback M.D. & Moos D., 1995. Fluid flow along potentially active faults in crystalline rock. *Geology*, 23(8), 683–686. https://doi.org/10.1130/0091-7613(1995)023<0683:FFAPAF>2.3.CO;2.

Chatterjee R. & Paul S., 2012. Estimation of in-situ stress from cleat orientation for coal bed methane exploration, Jharia Coalfield, India. [in:] *9th Biennial International Conference & Exposition on Petroleum Geophysics*, P-060.

Dawson G.K.W., Esterle J.S., Golding S.D. & Massarotto P., 2011. Cleat and joint intersections and mineralisation of a coal core from the Bowen Basin, Queensland, Australia. [in:] *The 3rd Asia Pacific Coalbed Methane Symposium, May 3–6, 2011, Brisbane, Australia*, 51.

Dershowitz W., Einstein H., LaPoint P., Eiben T., Wadleigh E. & Ivanova V., 1998. *Fractured reservoir discrete feature network technologies. Final report, March 7, 1996 to September 30, 1998*. United States. https://doi.org/10.2172/757228.

Jaeger J.C., Cook N.G.W. & Zimmerman R.W., 2007. *Fundamentals of Rock Mechanics*. Wiley-Blackwell, Chichester, UK.

Jureczka J., Ihnatowicz A. & Zdanowski A., 2019. Polskie zagłębia węgla kamiennego – zarys historii badań Państwowego Instytutu Geologicznego. *Przegląd Geologiczny*, 67(7), 578–583.

Kępiński M., 2020. Determination of stress state based on well logging data and laboratory measurements – a CBM well in the southeastern part of the Upper Silesian Coal Basin (Poland). *Geology, Geophysics & Environment*, 46(2), 77–92. https://doi.org/10.7494/geol.2020.46.2.77.

Kotas A., Kwarciński J. & Jureczka J., 1990. *Obliczenie zasobów metanu w pokładach węgla Górnośląskiego Zagłębia Węglowego oraz ocena możliwości pozyskania*. Narodowe Archiwum Geologiczne PIG-PIB, Warszawa, Poland.

Labourdette R., Hegre J., Imbert P. & Insalaco E., 2008. Reservoir-scale 3D sedimentary modelling: Approaches to integrate sedimentology into a reservoir characterization workflow. [in:] Robinson A., Griffiths P., Price S., Hegre J. & Muggeridge A. (eds.), *The Future of Geological Modelling in Hydrocarbon Development*, Geological Society, London, Special Publications, 309, 75–85.

Matheron G., Beucher H., de Fouquet C., Galli A., Guérillot D. & Ravenne C., 1987. Conditional simulation of the geometry of fluvio-deltaic reservoirs. [in:] *SPE Annual Technical Conference and Exhibition, September 27–30, 1987, Dallas, Texas*, SPE-16753-MS. https://doi.org/10.2118/16753-MS.

Milad B., Ghosh S., Suliman M. & Slatt R., 2018. Upscaled DFN models to understand the effects of natural fracture properties on fluid flow in the Hunton Group tight Limestone. [in:] *SPE/AAPG/SEG Unconventional Resources Technology Conference, Houston, Texas, USA, July 2018*, URTEC-2903038-MS. https://doi.org/10.15530/URTEC-2018-2903038.

Oda M., 1985. Permeability tensor for discontinuous rock masses. *Géotechnique*, 35(4), 483–495. https://doi.org/10.1680/geot.1985.35.4.483.

Palmer I. & Mansoori J., 1998. How permeability depends on stress and pore pressure in coalbeds: A new model. *SPE Reservoir Evaluation & Engineering*, 1(6), 539–544. https://doi.org/10.2118/52607-PA.

Reynolds M.M. & Shaw J.C., 2005. Optimizing hydraulic fracturing treatments for CBM production using data from post-frac analysis. [in:] *Canadian International Petroleum Conference, June 7–9, 2005, Calgary, Alberta*, PETSOC-2005-213. https://doi.org/10.2118/2005-213.

Rogers S.F., 2003. Critical stress-related permeability in fractured rocks. [in:] Ameen M.S. (ed.), *Fracture and In-situ Stress Characterization of Hydrocarbon Reservoirs*, Geological Society, London, Special Publications, 209, 7–16. https://doi.org/10.1144/GSL.SP.2003.209.01.02.

Sathar S., Reeves H.J., Cuss R.J. & Harrington J.F., 2012. The role of stress history on the flow of fluids through fractures. *Mineralogical Magazine*, 76(8), 3165–3177. https://doi.org/10.1180/minmag.2012.076.8.30.

Schlumberger, 2008. *Characterization of Fractured Reservoirs: Reliable, predictive models to optimize carbonate reservoir performance*. https://www.slb.com/-/media/files/theme/brochure/cb-characterization-09os0003.ashx [access: 21.03.2022].

Schlumberger, 2019. *Kinetix: Reservoir-centric stimulation-to-production software*. https://www.slb.com/completions/stimulation/stimulation-optimization/kinetix-reservoir-centric-stimulation-to-production-software [access: 1.05.2022].

Schlumberger, 2021. *Petrel User Assistance*.

Słoczyński T. & Drozd A., 2018. Methane potential of the Upper Silesian Coal Basin carboniferous strata – 4D petroleum system modeling results. *Nafta-Gaz*, 74(10), 703–714. https://doi.org/10.18668/NG.2018.10.01.

Snow D.T., 1969. Anisotropic Permeability of Fractured Media. *Water Resources Research*. 5(6), 1273–1289. https://doi.org/10.1029/WR005i006p01273.

Stopa J. & Mikołajczak E., 2018. Empirical modeling of two-phase CBM production using analogy to nature. *Journal of Petroleum Science and Engineering*, 171, 1487–1495. https://doi.org/10.1016/j.petrol.2018.07.018.

Xuanhe T., Haiyan Z., Qinqyou L. & Yuija S., 2019. A reservoir and geomechanical coupling simulation method: Case studies in shale gas and CBM reservoir. [in:] *International Petroleum Technology Conference, March 26–28, 2019, Beijing, China*, IPTC-19288MS. https://doi.org/10.2523/IPTC-19288-MS.

Zdanowski A. & Żakowa H. (eds.), 1995. *The Carboniferous System in Poland*. Prace Państwowego Instytutu Geologicznego, 148, PIG, Warszawa.

Zheng S. & Xue L., 2011. Modelling and simulation of a new dual porosity CBM reservoir model with an improved permeability model through horizontal wells. [in:] *SPE Middle East Unconventional Gas Conference and Exhibition, January 31–February 2, 2011, Muscat, Oman*, SPE-141118-MS. https://doi.org/10.2118/141118-MS.

Zoback M.D., 2007. *Reservoir Geomechanics*. Cambridge University Press, Cambridge.

Zoback M.D., Barton C.A., Brudy M., Castillo D.A., Finkbeiner T., Grollimund B.R., Moos D.B. et al., 2003. Determination of stress orientation and magnitude in deep wells. *International Journal of Rock Mechanics and Mining Sciences*, 40(7–8), 1049–1076. https://doi.org/10.1016/j.ijrmms.2003.07.001.